ChemPubSoc Europe

DOI: 10.1002/cctc.201800921

CHEMCATCHEM Full Papers

Improved Cyclohexane Oxidation Catalyzed by a Heterogenized Iron (II) Complex on Hierarchical Y Zeolite through Surfactant Mediated Technology

Vanmira Van-Dúnem,[a] Ana P. Carvalho,*[b] Luísa M. D. R. S. Martins,*[c] and Angela Martins*[a, b]

The hydrotris (pyrazol-1-yl) methane iron (II) complex [$FeCl_2$(Tpm)] [Tpm = $HC(C_3N_2H_3)_3$] was successfully immobilized, by the incipient wetness impregnation method, in parent and hierarchical Y zeolite modified through surfactant mediated methodology using different bases (NH_4OH, NaOH or TPAOH). The catalytic performance and recyclability of supported Fe complex was evaluated in the oxidation of cyclohexane with hydrogen peroxide to cyclohexanol and cyclohexanone under mild conditions and two distinct behaviors were observed: using commercial Y and modified Y with NaOH the complex is anchored mainly at the outer surface of the zeolite supports, resulting in high lixiviation after the first catalytic cycle. When NH_4OH and TPAOH are used during the zeolite treatments the particular textural parameters exhibited by these two supports are able to effectively retain the complex molecules, resulting in a high recyclability observed after three consecutive cycles, especially when NH_4OH treated zeolite was used as support.

Introduction

Efficient catalytic oxidation of alkanes into high value functionalized products under sustainable conditions remains challenging.[1–4] Limitations of the usage of alkanes as raw materials, in view of their inert character, are harsh reaction conditions, low product yield and/or low selectivity. Therefore, the development of efficient catalytic systems under environmentally benign conditions for selective oxidation of alkanes is highly demanding.

An exemplary large-scale building block industrial production is the oxidation of cyclohexane. Although economically very important in view of the significance of the oxidized product [KA oil, the cyclohexanol (A) and cyclohexanone (K) mixture] for the manufacturing of adipic acid and caprolactam (precursors to polyamides widely used in several industries), the current industrial process for cyclohexane oxidation is inefficient (*ca.* 10% conversion; 85% selectivity).[5] Therefore, there is an urgent need to develop selective and energy efficient direct alkane oxidation chemistry that could lead to environmental and economically superior catalytic processes and allow natural resources to be used more efficiently as feed-stocks for chemicals.

Like the active centers of some enzymes (*e.g.* particulate methane monooxygenase), transition metal complexes can potentially activate and functionalize the inert C–H bonds of hydrocarbons with high atom economy and low energy under mild reaction conditions.[6,7] Lately, bio-inspired catalysts with available, non-toxic and inexpensive first row transition metal centers were designed to act as selective and effective homogenous catalysts in C–H activation reactions at r.t. and using the environmentally benign hydrogen peroxide as oxidant.[8–12] However, the above homogeneous catalysts lack in reusability.

Thus, the knowledge that immobilization of such catalysts on solid supports could be a strategy to combine the high catalytic activity of homogeneous catalysts with the easy separation and recycling ability of the heterogeneous ones, prompted us to follow such approach. Several materials were already used as supports to anchor homogeneous catalysts, particularly C-scorpionate complexes, such as functionalized silica[13] carbon materials,[14,15] polymers,[16] and zeolites.[17] The zeolite materials present some advantages over other supports due to their mechanical stability, high porosity and controlled acidity, which makes them particularly attractive as hosts for encapsulation of metal complexes.[18–20] However, the purely microporous nature of these materials can be a drawback when large molecules are involved, or the immobilization of large homogeneous catalysts is pretended.[21] One of the strategies to overcome the limitation inherent to zeolites is the introduction of mesoporosity through several methods that can be applied during or post-synthesis, leading to the creation of hierarchical

[a] *V. Van-Dúnem, Dr. A. Martins*
ADEQ, Instituto Superior de Engenharia de Lisboa IPL
Rua Conselheiro Emídio Navarro 1, 1959-007 Lisboa (Portugal)
E-mail: amartins@deq.isel.ipl.pt
[b] *Dr. A. P. Carvalho, Dr. A. Martins*
Centro de Química e Bioquímica and Centro de Química Estrutural, Faculdade de Ciências
Universidade de Lisboa, 1749-016, Lisboa (Portugal)
E-mail: apcarvalho@fc.ul.pt
[c] *Prof. L. M. D. R. S. Martins*
Centro de Química Estrutural, Instituto Superior Técnico
Universidade de Lisboa
Av. Rovisco Pais 1049-001 Lisboa (Portugal)
E-mail: luisamargaridamartins@tecnico.ulisboa.pt

Supporting information for this article is available on the WWW under https://doi.org/10.1002/cctc.201800921

This manuscript is part of a Special issue on the "Portuguese Conference on Catalysis" based on the International Symposium on Synthesis and Catalysis (ISySyCat).

zeolites.[22,23] Desilication is one of the most common and simple methods to create mesoporosity and was successfully applied to several zeolite structures, such as MFI,[24,25] MOR,[26,27] BEA[28] or MWW[29] to explore their action as catalysts or catalyst supports.[30] The catalytic behavior of [$FeCl_2$(Tpm)] [Tpm = $HC(C_3N_2H_3)_3$] immobilized on desilicated MOR zeolite for the peroxidative oxidation of cyclohexane to KA oil was studied by us in a previous work.[17] It was found that the complex immobilized on desilicated MOR is more efficient (higher TON, yield values and lower loading of oxidant) when compared to the same catalyst anchored on commercial MOR, or to the homogeneous C-scorpionate iron catalyst.[31] However, it was also found that after the first catalytic run a loss of 54% of catalysts occurs, attributed to lixiviation. In fact, the textural analysis of MOR supports before and after immobilization pointed out that at least a fraction of the complex must be located at the external surface of the crystals. Indeed, it was already reported that one of the disadvantages of conventional desilication is the poor control of the mesoporosity, namely the size, shape, connectivity and the location of the mesopores, especially when strong bases, like NaOH, are used.[29] One of the current trends in the research of hierarchical zeolites consists in provide different methods aiming at controlling hierarchical porosity, such as the combination of a based (*e.g.* NaOH) with a surfactant. This methodology was deeply explored by Garcia Martinez *et al.*,[32,33] who reported a surfactant-templating process for introducing highly-controlled mesoporosity. Under adequately selected experimental conditions (*e.g.* concentration, temperature, time and pH) the silica dissolution takes place just locally and the surfactant micelles lead to the rearrangement of the released zeolite subunits into an ordered mesostructure. The global result is the appearance of ordered mesopores within the zeolite crystals. Garcia-Martinez group applied this strategy to produce hierarchical Y zeolite using NH_4OH base solution and cetyltrimethylammonium bromide (CTAB) surfactant, followed by a thermal treatment under autogenous pressure.[34] According to the authors, the treated Y zeolite exhibits not only a higher mesoporosity but its mesopore size distribution was much more uniform, and the crystal size and morphology were preserved after treatment. In this work we prepared a hierarchical Y zeolite based on the above methodology[32,34] using experimental conditions, namely base concentration, used in our previous work.[26] The objective was to study the influence of other bases such as NaOH and tetrapropylammonium hydroxide (TPAOH) on the textural properties of the treated samples, explore the application of such hierarchical Y materials as supports for the heterogenization of the C-scorpionate iron (II) [$FeCl_2$(Tpm)] catalyst and evaluate the performance of the heterogenized species for the peroxidative oxidation of cyclohexane to KA oil. We aim at taking advantage of the regular mesoporosity of mesostructured Y zeolite which, desirably, prevents the extended lixiviation of the active species and allows a large number of catalytic cycles when compared to commercial and conventionally desilicated zeolites.

Results and Discussion

The hydrotris (pyrazol-1-yl) methane iron (II) complex [$FeCl_2$(Tpm)] [Tpm = $HC(C_3N_2H_3)_3$] (**Fe**) was promptly synthesized by reaction of iron chloride with Tpm scorpionate, according to a known procedure,[31] and immobilized, by the incipient wetness impregnation method, in parent Y zeolite and hierarchical mesoporous Y pretreated with different bases, **Fe**@Y_B (B = NH_4OH, NaOH or TPAOH), as depicted in Scheme 1.

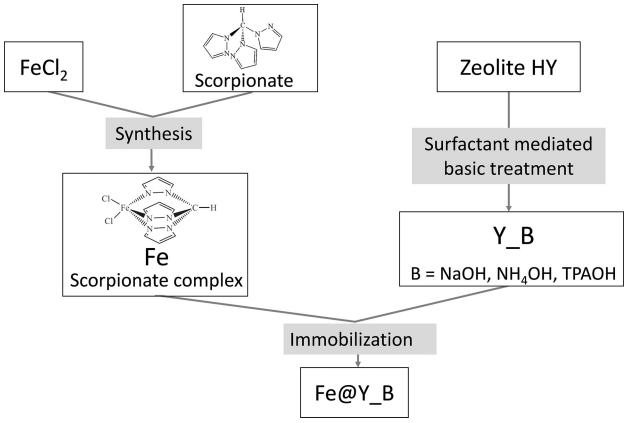

Scheme 1. Samples preparation methodology.

Physicochemical Characterization

The X-ray diffraction patterns of parent and treated samples (see Figure S1 in Supplementary Information) reveal a long-range crystal ordering in all the cases, since there are no important changes in peak positions. To quantify structural modifications, the degree of crystallinity C_{XRD} was estimated following the procedure described in ASTMD 3906–03[35] *i.e.* by performing the ratio between the areas of the diffraction peaks corresponding to the crystallographic planes (331), (333), (440), (533), (648), (660), (555) and (664) of the treated samples and parent Y, the later been used as reference. Peaks integration was made using the "Peak-fit" software. All the samples present a degree of crystallinity above 90%, independently of the base used, pointing out that the surfactant mediated methodology followed allows to preserve the structural properties of the materials in a large extend. Sample Y_NaOH_P, treated in identical experimental conditions as sample Y_NaOH, but in the absence of CTAB, also retained a high degree of crystallinity (89%), showing that, from the structural point of view, the two procedures lead to similar results. On the contrary, when the structure is modified under autogenous pressure created in the autoclave, the lack of CTAB in the reaction mixture (sample HY_NaOH_A) resulted in an amorphous material.

Upon the complex immobilization on the zeolitic supports no significant changes in the X-ray patterns were observed when compared with the correspondent supports.

SEM micrographs for parent and treated zeolite supports are displayed in Figure 1. For the parent material the image shows crystals with shape and size typical of Y zeolite. Upon treatments the crystals maintain the characteristic shape and size, however, some fragmentation and accumulation of debris at the crystal surface is visible, especially in the case of Y_TPAOH and Y_NaOH. In this later case it is clearly visible some degradation and perforation of the crystals, as expected, since NaOH is a stronger base. On the other hand, the micrograph of sample Y_NH_4OH seems to demonstrate that the treatments did not damage the crystals.

Figure 2 shows TEM images of parent and treated supports. The parent Y zeolite seems to present already some degradation of the crystals borders as denoted by the lighter zones, which can be attributed to the acid washing with citric acid prior to the alkaline + surfactant treatment. When comparing the three treated materials it is clear that Y_NaOH sample presents a higher density of lighter zones, suggesting that the crystals were more damaged by the stronger NaOH base.

However, when comparing the lighter patterns of this sample with the ones that can be visualized on, for example, MOR samples desilicated using NaOH with the same concentration[17], it appears that, in the present work the patterns are more homogeneous, which denotes the role of the surfactant molecules to control the mesopore size distribution. In the case of Y_NH_4OH and Y_TPAOH the crystals are denser when compared with Y_NaOH sample, denoting a more controlled extension of crystals deterioration by the bases. This can be explained by the softener character of these compounds in comparison with NaOH, but also to a more effective role of the surfactant molecules. In fact, the lighter zones present on the crystals, exhibit some homogeneous round shapes that may evidence the crystal rearrangement around CTAB micelles, originating the mesopores.

The N_2 adsorption-desorption isotherms at −196 °C of the parent Y zeolite and the materials obtained after alkaline treatment and immobilization are shown in Figure 3 and Figure S2. All the curves can be classified as type I + IV

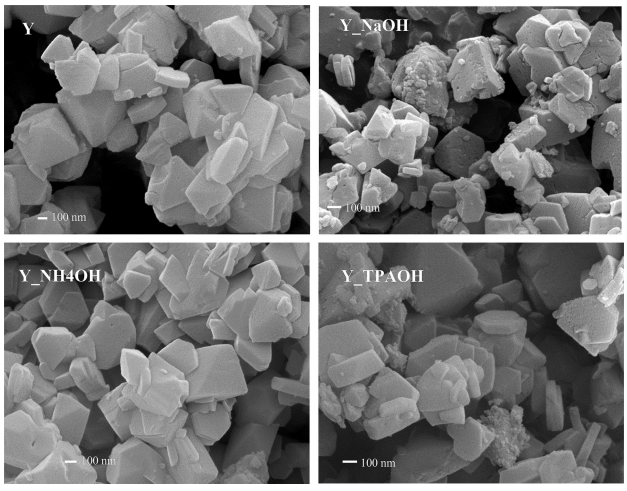

Figure 1. SEM images of parent and treated zeolitic supports.

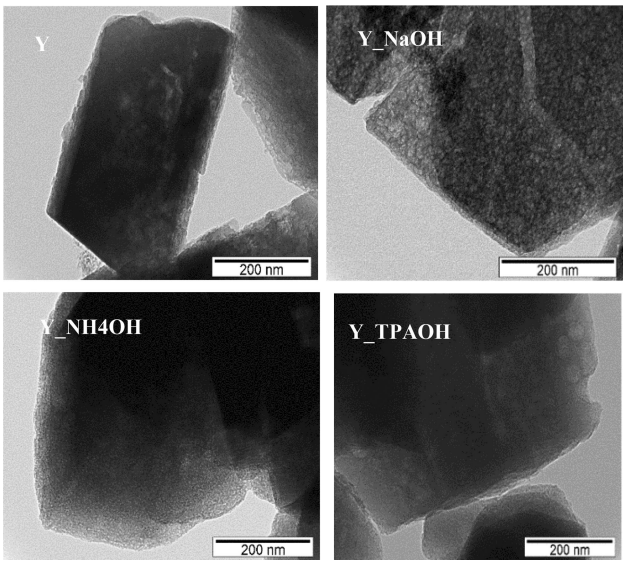

Figure 2. SEM images of parent and treated zeolitic supports.

isotherms[36] denoting a marked microporous nature typical of zeolitic structures, along with a mesopore network.

The presence of some mesoporosity in the starting material may result from the aggregation of the crystals, although some structural changes promoted by the citric acid treatment cannot be disregarded, as suggested by TEM micrographs. From the analysis of the isotherms configuration it turns clear that, under the experimental conditions studied, the base used influences the textural changes since, in the case of samples treated with NH_4OH and TPAOH, a smooth step is observed in the p/p^0 range of around 0.3 and 0.5, which is not observed in the isotherms of the NaOH treated material. Lastly, as expected, a significant impact of the treatments on the mesoporosity development is demonstrated by the accentuated upward deviation of the curves at high p/p^0 values, and by the H4 hysteresis loops.

Although the X-ray diffraction results shown no benefit of the surfactant mediated process in comparison with the more conventional methodology, the results presented in Figure S3 show that the presence of CTAB in the reaction medium lead to a different textural evolution, namely to a more extensive mesoporosity development.

The quantitative analysis of the microporosity was made applying the α_S method using as reference the isotherm obtained on non-porous silica.[37] In the case of samples Y and Y_NaOH, the α_S curves present two consecutive linear regions, the first defined by the experimental points determined at $0.02 > p/p^0 > 0.4$, and the second by data obtained at $p/p^0 > 0.4$, *i.e.* multilayer region. These are the usual features of zeolites' α_S plots[26] which are interpreted as pointing out the presence of a large volume of narrow micropores, *i.e.* ultramicropores (V_{ultra}–$\phi < 0.7$ nm) characteristic of the zeolite framework, and also larger micropores, *i.e.* supermicropores (V_{super}–0.7 nm $> \phi >$ 2 nm). The volume of the latter are determined through the expression $V_{super} = V_{micro} - V_{ultra}$, being V_{micro} the total micropore

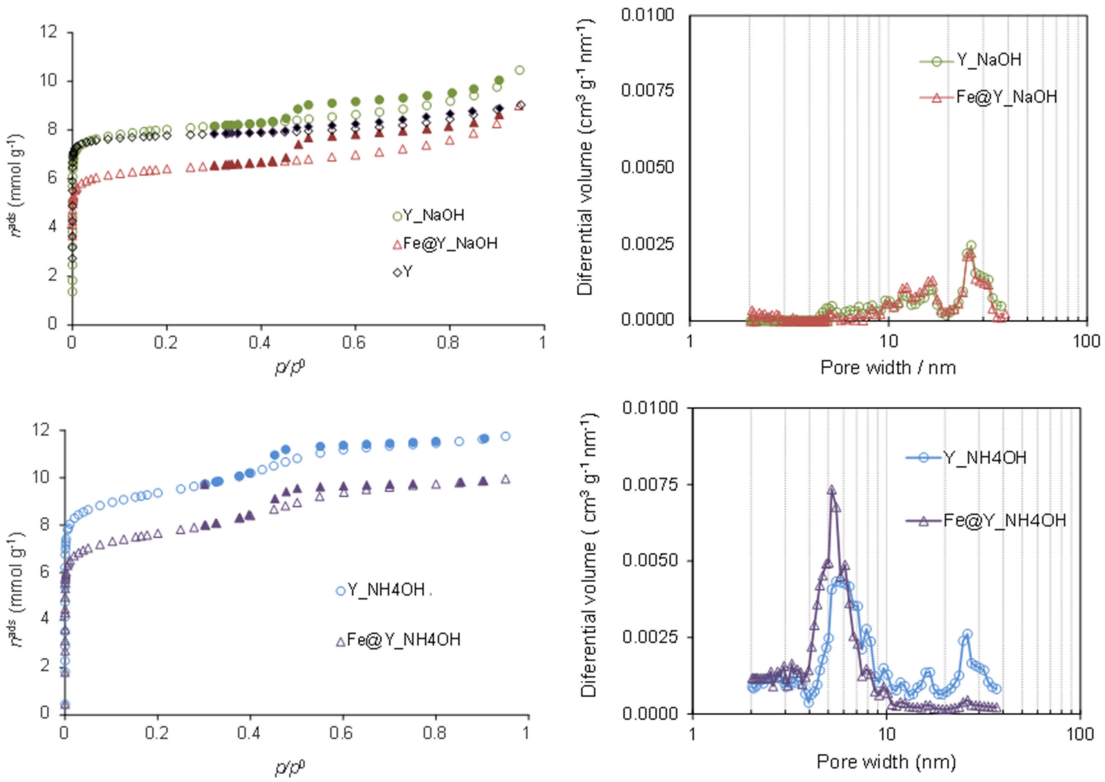

Figure 3. N_2 adsorption desorption isotherms (left) and mesopore size distributions (right).

volume obtained by back extrapolation of the multilayer region.

Due to the differences in the isotherms configuration previously discussed, the α_s plots of samples Y_NH_4OH and Y_TPAOH are more complex exhibiting three linear regions. The first region extends up to α_s values *ca.* 0.90 ($p/p^0 \approx 0.35$), followed by a steeper linear region up to α_s *ca.* 1.1 ($p/p^0 \approx 0.5$) after what the linear branch of the multilayer region is observed (see Fig S4). Taking into account that the supermicropores filling process occurs in the relative pressure range of 0.1–0.15[38] we may conclude that in these cases the difference of the volumes obtained by back extrapolation of the first and the multilayer linear regions will correspond the volume of supermicropores and also narrow mesopores. To distinguish this situation, in Table 1 the values are written in bold.

Table 1. Textural parameters, expressed in $cm^3\ g^{-1}$, estimated from the analysis of the N_2 isotherms. For parameter's symbol designation see text.

Sample	V_{ultra}	V_{super}	V_{meso}
Y	0.24	0.02	0.06
Y_NaOH	0.22	0.02	0.13
Y_NH_4OH	0.23	**0.11**	0.07
Y_TPAOH	0.22	**0.11**	0.05
Fe@Y	0.19	0.02	0.04
Fe@Y_NaOH	0.17	0.02	0.13
Fe@Y_NH_4OH	0.18	**0.09**	0.05
Fe@Y_TPAOH	0.19	**0.09**	0.06

The volume denoted as V_{meso} was calculated from the difference between the total pore volume, considered as the N_2 uptake at $p/p^0 = 0.95$, and the volume corresponding to the positive intercept of the multilayer region. No mass correction was made in the case of immobilized catalysts due to the very small amount of complex retained.

The values reported in Table 1 demonstrate that upon the alkaline treatment the volume of the narrower micropores, V_{ultra}, presents always a small decrease, showing that the micropore network was preserved in a large extend, what is in accordance with the high crystallinity values determined by XRD data. The development of larger porosity seems to be dependent of the base used since while for Y_NaOH there is a clear increase of V_{meso}, for the other two samples the results indicate that the most important change corresponds to the increase of the wide micropores and small mesopores (values in bold in Table 1). This different evolution is also pointed out by the mesopore size distributions obtained by the DFT method (Figures 3 and S2). The results reveal that while for sample Y_NaOH the mesoporosity corresponds mainly to pores of width higher than 10 nm, for samples Y_TPAOH and, especially Y_NH_4OH a clear bimodal distribution is observed with a large volume of pores in the range of 4 to 10 nm and a second less intense peak at corresponding to pores with widths larger than 10 nm.

The complex immobilization resulted in all the cases in a small decrease of the microporosity characteristic of the zeolitic structure, V_{ultra}. On the other hand, when considering the effect of the immobilization on larger porosity we observe that in the

case of samples **Fe**@_Y and **Fe**@Y_NaOH the values of V_{super} and V_{meso} are practically the same of those presented by the supports pointing out that the complex must be dispersed on the crystals outer surface resulting in the blockage of some pore apertures, thus leading to the decrease of V_{ultra} values. The comparison of the predicted dimensions of the complex (maximum width 0.8 nm)[17] and the micropore diameter of the Y zeolite is 7.4 Å (12 member oxygen ring apertures) supports this hypothesis.

The other two catalysts, **Fe**@Y_NH_4OH and **Fe**@Y_TPAOH were obtained from supports where the volume corresponding to supermicropores and narrow mesopores is very important. In this case the results indicate that, at least a fraction of the complex will be located in this porosity (compare the values in bold in Table 1 for samples before and after complex immobilization).

Table 2. Selected data[a] for the optimized oxidation of cyclohexane with hydrogen peroxide catalyzed by **Fe**@Y_B (B = NH_4OH, NaOH or TPAOH).

Entry	Catalyst	Yield [%][b] Cyclohexanol	Cyclohexanone	Total	Total TON[c]
1	**Fe**@Y	13.6	4.5	18.1	45
2	**Fe**@Y_TPAOH	23.5	4.2	27.7	69
3	**Fe**@Y_NaOH	26.6	7.6	34.2	86
4	**Fe**@Y_NH_4OH	19.9	5.7	25.6	64
5	**Fe**@Y_NaOH[d]	20.9	6.2	27.1	271
6	Y or Y_B	0	0	0	0
7	–	0	0	0	–

[a]Reaction conditions: cyclohexane (5 mmol), catalyst (20 μmol, based on the iron complex **Fe**, 0.4 mol% *vs.* cyclohexane), H_2O_2 (50% aq., 10 mmol) *n*(Hpca)/*n*(catalyst) = 12.5, 24 h, in acetonitrile (3 mL) at r.t.. Amounts of cyclohexanone (K) and cyclohexanol (A) were determined by GC analysis after reduction of the aliquots with solid PPh_3[39] using $MeNO_2$ as standard. [b]Percentage molar yield [(mol of product)/(mol of cyclohexane)]. [c]Total turnover number, defined as mol of A and K/mol of **Fe**. [d]5 μmol of catalyst.

Catalytic Oxidation of Cyclohexane

The catalytic activity of the C-scorpionate iron (II) complex [$FeCl_2$(Tpm)] [Tpm = $HC(C_3N_2H_3)_3$] immobilized at the above hierarchical mesoporous Y zeolite pretreated with different bases, **Fe**@Y_B (B = NH_4OH, NaOH or TPAOH), was evaluated for the oxidation of cyclohexane, by aqueous H_2O_2, to KA oil (cyclohexanol and cyclohexanone), at room temperature, in a slightly acidic (pyrazine carboxylic acid, Hpca) acetonitrile medium, according to the Scheme 2.

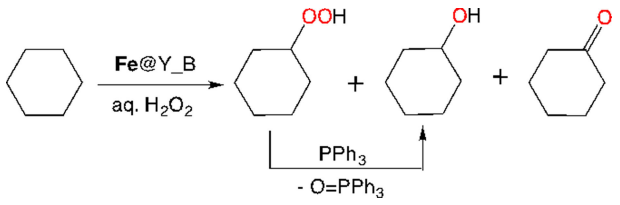

Scheme 2. Oxidation of cyclohexane to cyclohexanol and cyclohexanone catalyzed by **Fe**@Y_B (B = NH_4OH, NaOH or TPAOH).

The hybrid materials act as efficient reusable catalysts for the above oxidation, leading to a maximum KA oil yield of 34% and to turnover numbers (TONs) up to 271 (Table 2, entries 3 and 5). Their catalytic performances were compared, in terms of products yield, turnover number (TON) and selectivity as a function of the support and reaction conditions (*e.g.*, time, temperature, type and amount of oxidant or catalyst loading).

No cyclohexane oxidation by hydrogen peroxide took place in the absence of **Fe** (Table 2) or the oxidant. The use of hydrogen peroxide revealed to be preferable (besides environmental issues) to, *e.g.*, *tert*-butylhydroperoxide, TBHP since the latter, under identical conditions, affords much lower KA oil yields (e.g., 13.8% for **Fe**@Y_NaOH) with low selectivity (*e.g.*, diols were detected by GC-MS analysis of the final reaction mixture). Moreover, the amount of hydrogen peroxide used affects the overall yield of products: 50% aq. H_2O_2 proved being more effective than the 30% aq. solution.

Increasing the temperature from r.t. to 75 °C, a drastic KA oil yield decrease is observed (*e.g.*, for **Fe**@Y_NaOH the 34.2% yield reached at r.t. dropped to 6.0% at 75 °C, while maintaining all the other reaction conditions), conceivably on account of the decomposition of H_2O_2.

The effect of the amount of catalyst was also investigated. The total yield was enhanced by increasing the load of catalyst until a **Fe** amount of 20 μmol.

At the optimized reaction conditions (Table 2), no traces of by-products were detected by GC analysis of the final reaction mixtures, indicating the high selectivity towards the formation of cyclohexanol and cyclohexanone, easily controllable in our catalytic systems.

The yields obtained at the optimized conditions are comparable to those achieved by the same iron complex heterogenized on mesoporous mordenite, desilicated by the conventional method (MOR–D),[17] although a longer reaction time is requested in the present study.

The primary advantage of **Fe**@Y_B catalysts, in particular of **Fe**@Y_NH_4OH and **Fe**@Y_TPAOH, relative to **Fe**@MOR–D is their stability under the reaction conditions, allowing their recovery at the end of the catalytic cycle and re-use in a consecutive one. In fact, as mentioned above, after the first catalytic run, 54% of **Fe**@MOR–D undergone lixiviation.[17]

The re-usability in consecutive cycles of **Fe**@Y_B is depicted in Figure 4.

In the 2nd cycle, whereas **Fe** immobilized at the commercial Y, **Fe**@Y, loses *ca.* 57% of its initial activity, **Fe**@Y_NH_4OH and **Fe**@Y_TPAOH, advantageously, present much higher stability (maximum activity loss of 11%). On the other hand, **Fe**@Y_NaOH exhibits a stability trend similar to **Fe**@Y.

The observed recycling behavior of **Fe**@Y_B appears to be resulting from the porosity differences found in the samples modified template mediated basic treatment. Actually, the textural characterization results previously discussed, pointed out that, in the case of catalysts **Fe**@Y and **Fe**@Y_NaOH the complex must be located mainly in the crystals' outer surface, thus more prone to leaching, especially in the case of the **Fe**@Y. The results also indicated that in the other two catalysts (**Fe**@Y_

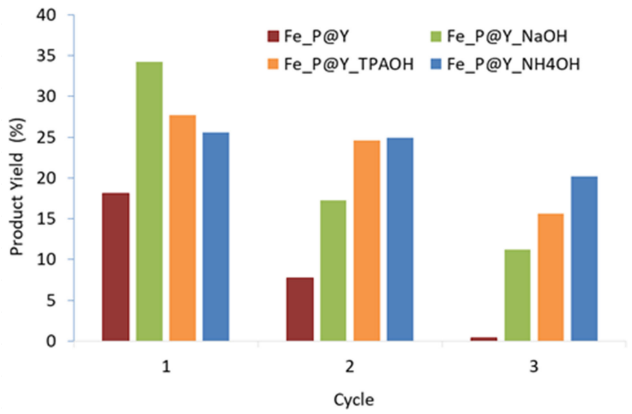

Figure 4. Effect of **Fe**@Y_B (B = NH_4OH, NaOH or TPAOH) recycling on the products yield of cyclohexane oxidation with hydrogen peroxide.

NH_4OH and **Fe**@Y_TPAOH) at least a fraction of the complex is located on the porosity formed by the wider micropores and narrow mesopores. Considering the performance of these two catalysts in the re-use assays and bearing in mind that the maximum width of the scorpionate complex is 0.8 nm[17], we may hypothesize that most probably it is immobilized in the wider microporosity where the interaction with the support is enhanced.

To rationalize the catalytic behavior of **Fe**@Y_NH_4OH, fresh and recovered (after the 1st and 3rd catalytic cycles) catalysts were characterized by XPS. The survey spectra of the fresh catalyst (Figure 5) exemplifies the results obtained showing

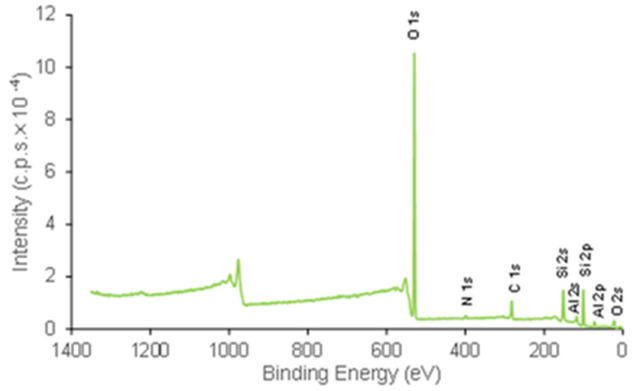

Figure 5. XPS survey spectrum of sample Fe@Y_NH_4OH.

that, as expected, oxygen, silicon and carbon are the main elements detected. Small peaks also show the presence of nitrogen and aluminum. Iron is also detected as a very low intensity peak. Survey spectra of re-used catalyst are presented in Figure S4.

The comparison of the surface composition of the various samples (Table 3) shows that, after use, the catalysts present a significant decrease of silicon and oxygen content along with an important increase of carbon and nitrogen contents. This evolution may be due to the presence adsorbed species on the catalysts surface, *i.e.*, either reagents or products molecules, or

Table 3. Surface contents of fresh **Fe**@Y_NH_4OH catalysts and samples recovered after the 1st and 3rd catalytic cycles, and Fe global amount determined by ICP (numbers in bold).[a]

Element [mmol g^{-1}]	Fresh	1st cycle	3rd cycle
Si	11.7	6.3	4.8
O	30.1	23.0	19.7
Al	2.6	2.0	1.4
C	7.7	20.2	25.2
N	0.6	2.0	2.5
Fe	0.17	0.20	0.11
Fe	**0.09**	**0.11**	**0.09**

[a]Surface contents determined from XPS atomic percentages: mmol X/g = atomic % X /(Σ[atomic % (i) × Ar(i)].

acetonitrile (used as solvent) or nitromethane (used as internal standard for the chromatographic analysis). The almost absent adsorption capacity observed in both re-used samples (data not shown) supports this explanation hypothesis, as well as the dark color of the samples after the catalytic assays.

In the case of Fe, the results gathered allow the comparison of the global and surface composition. The data obtained with the fresh catalyst demonstrate that the complex is not homogenously dispersed in the solid matrix being preferentially located in the external surface of the crystals, what is in accordance with the decrease of the textural parameters previously discussed. The use of the sample in the catalytic reaction resulted only on a small decrease of the surface Fe content in the case of the sample obtained after the 3rd catalytic cycle. Moreover, the results from the hot filtration test (see experimental) have shown that after removal of **Fe**@Y_NH_4OH, the reaction did not proceed indicating that no catalytically active iron compound remained in the filtrate.

To gather deeper information on the iron oxidation states Fe 2p XPS spectra were performed.

The results are depicted in Figure 6, showing that, as a consequence of the catalytic use, a broad peak at *ca.* 730 eV is perceptible. This peak, that is absent in fresh catalyst spectrum, corresponds to Fe^{3+}.[40,41] The other two peaks common to all spectra are much more defined and are assigned to Fe^{2+} (722 eV) and $Fe^{2+} + Fe^{3+}$ (709 eV and 711 eV, respectively, resulting in a broad peak).[38,39] The predominance of the Fe^{2+} oxidation state is in accord with the regeneration of the initial (before the catalytic reaction) oxidation state of the catalyst through the known redox Weiss reactions involved in the cyclohexane oxidation mechanism (Scheme 3)[8] and explains the catalytic performance of this material.

Conclusions

This study contributed to the development of stable and reusable heterogenized catalytic systems based on the immobilization of a transition Fe complex on hierarchical Y zeolite modified through template mediated methodology. For the preparation of the supports it was demonstrated that, under the experimental conditions used, the base type (NaOH, NH_4OH or TPAOH), in association with the surfactant molecules,

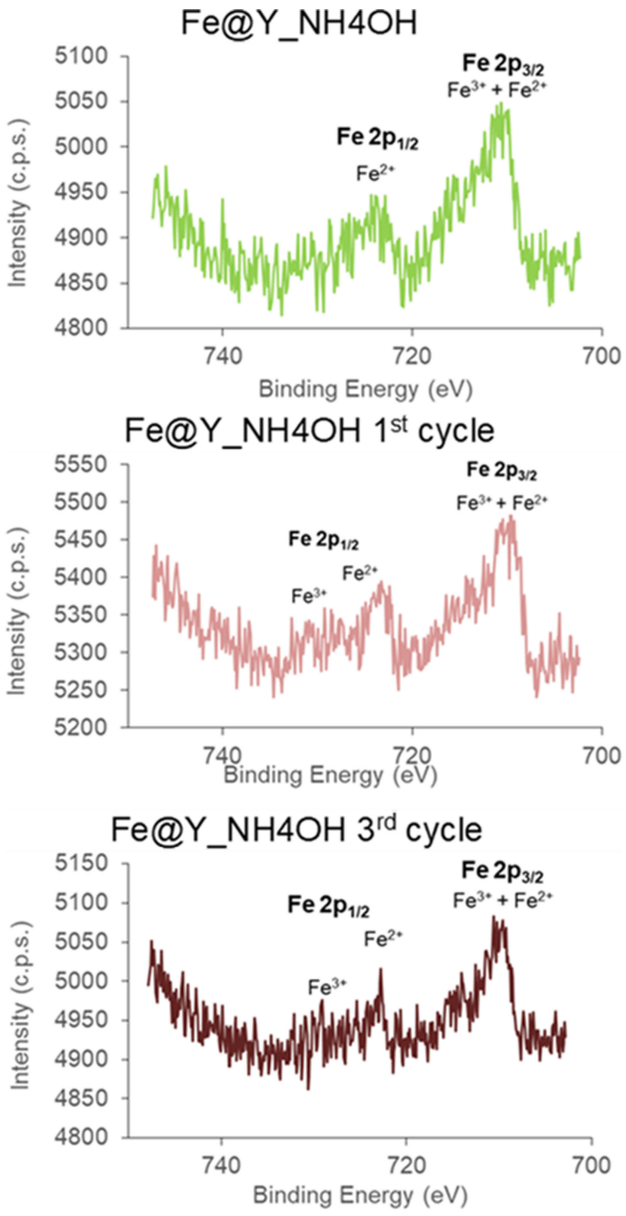

Figure 6. Fe 2p XPS spectra of fresh and used **Fe**@Y_NH_4OH catalysts.

strongly affected the textural properties of the materials, which influenced the immobilization of Fe complex in the supports. In the case of **Fe**@Y and **Fe**@Y_NaOH the complex is immobilized mainly at the crystals external surface which resulted in some blockage of pore apertures and significant complex leaching upon the first catalytic cycle. On the other hand, for **Fe**@Y_NH_4OH and **Fe**@Y_TPAOH the particular textural properties of these samples, comprising a large volume of wider micropores and narrow mesopores, allowed a more effective interaction between the complex and the support which resulted in the reusability of the catalyst for three consecutive cycles, especially in the case of **Fe**@Y_NH_4OH, where no significant product yields were lost after the third cycle. Finally, this study demonstrates that a fine tuning of the support textural properties can have a strong influence on the interaction between the catalyst and the support with important consequences on the catalytic

$$[Fe^{(II)}] + H_2O_2 \rightarrow HO\bullet + [Fe^{(III)}] + HO^- \quad (1)$$

$$[Fe^{(III)}] + H_2O_2 \rightarrow HOO\bullet + H^+ + [Fe^{(II)}] \quad (2)$$

$$HO\bullet + CyH \rightarrow H_2O + Cy\bullet \quad (3)$$

$$Cy\bullet + O_2 \rightarrow CyOO\bullet \quad (4)$$

$$CyOO\bullet + H_2O_2 \rightarrow CyOOH + HOO\bullet \quad (5)$$

$$CyOOH + [Fe^{II}] \rightarrow CyO\bullet + HO^- + [Fe^{III}] \quad (6)$$

$$CyOOH + [Fe^{III}] \rightarrow CyOO\bullet + H^+ + [Fe^{II}] \quad (7)$$

$$CyO\bullet + CyH \rightarrow CyOH + Cy\bullet \quad (8)$$

$$2CyOO\bullet \rightarrow CyOH + Cy_{-H}{=}O + O_2 \quad (9)$$

Scheme 3. Proposed oxidation mechanism for the oxidation of cyclohexane catalyzed by immobilized Fe.

behavior and recycling. In this sense, in a following study the influence of the base concentration on the support textural properties, as well as the effect of the support acidity on the complex immobilization and catalytic behavior will be addressed.

Experimental Section

Preparation of the Iron Complex [$FeCl_2\{\kappa^3$-$HC(C_3N_2H_3)_3\}$]

The hydrotris (pyrazol-1-yl) methane [$HC(C_3N_2H_3)_3$, Tpm] as well as the iron complex [$FeCl_2\{\kappa^3$-$HC(C_3N_2H_3)_3\}$] were prepared according to the literature.[31,42]

Preparation of the Zeolitic Supports

The parent material used as support was a faujasite structure (FAU), supplied by Zeolyst International (CBV500; lot 5000 N00322B), that according to the technical report has a $SiO_2/Al_2O_3 = 5.2$. The zeolites samples were modified through an alkaline treatment assisted by surfactant under autogenous pressure, according to the procedure described by Garcia-Martinez *et al.*[29] Prior to the treatments, 1 g of the parent zeolite was submitted to an acid wash with 1 mmol of citric acid (Sigma-Aldrich, 99.5% purity), using a suspension 10 wt.% for 1 h at 25 °C. The washed material was stirred with 64 mL of a 0.37 M solution of NH_4OH (Sigma-Aldrich, ≥25% NH_3 in H_2O) and 0.70 g of cetylmethylammonium bromide, CTAB, (Sigma, 99%) during 20 min at 25 °C. During this procedure the pH was measured and, if needed, a 2 M HCl (Aldrich, 37%) solution was added in order to keep the pH = 10. The mixture was then placed in stainless steel PTFE lined autoclaves and heated at 150 °C under autogenous pressure for about 10 h. The solid was recovered by centrifugation, washed and dried overnight at 80 °C. To remove the occluded surfactant the material was calcined at 550 °C under dry air atmosphere with a heating ramp of 5 °C/min during 2 h. The same procedure was used to prepare other two samples but using different bases: tetrapropylammonium hydroxide, TPAOH 0.2 M, (Sigma-Aldrich, 1 M in H_2O solution) and NaOH 0.2 M (Aldrich, p.a). In this later case the solid was submitted to an ion exchange with 2 M NH_4NO_3 (Sigma-Aldrich, ≥98%) solution for 6 h at 80 °C in order to remove some Na^+ exchanged during the treatment with

NaOH. The following was used to name the supports: Y_B (B = used base).

For comparison purposes two samples were treated with NaOH under experimental conditions similar to those described above, using the same concentration and duration of the treatment, but in the absence of surfactant. The materials will be designated as Y_NaOH_P and Y_NaOH_A to highlight the heating methodology followed: P – heating plate at 80 °C; A – autoclaved at 150 °C.

Immobilization of the Iron Complex [$FeCl_2\{\kappa^3$-$HC(C_3N_2H_3)_3\}$]

The iron complex [$FeCl_2\{\kappa^3$-$HC(C_3N_2H_3)_3\}$], designated as **Fe**, was immobilized by the incipient wetness impregnation method. **Fe** (0.018 g, 0.053 mmol) was dissolved in a previously determined amount of water needed to wet the support. The solution was slowly added and constantly mixed with 0.3 g of the support until a homogeneous paste was obtained, then the paste was dried, firstly at ambient temperature overnight and then at 50 °C in an oven for *ca.* 4 h. The samples will be designated as **Fe**@_Y_B (B = used base).

Physicochemical Characterization

The structural characterization of the supports and **Fe** loaded samples was carried out by powder X-ray diffraction (XRD) using a Pan'Analytical PW3050/60X'Pert PRO ($\theta/2\theta$) equipped with X'Celerator detector and with automatic data acquisition (X'Pert Data Collector (v2.0) software using a CuKα radiation as incident beam, 40 kV-30 mA. Diffractograms were obtained by continuous scanning from 5° to 40° 2θ, with a step size of 0.02° 2θ and a time step of 0.4 s. Far infrared spectra (400–200 cm^{-1}) were recorded on a Vertex70 spectrophotometer, in CsI pellets. In selected samples, the metal content present on the immobilized complexes were analyzed by ICP using a ICP-AES Horiba Jobin-Yvon model Ultima equipment at Laboratório de Análises, IST Lisbon, Portugal. XPS analysis was performed at CEMUP on a Kratos AXIS Ultra HAS equipment, with VISION software for data acquisition and CASAXPS software for data analysis. The effect of the electric charge was corrected by reference to the carbon peak (284.6 eV). Scanning and transmission electron microscopy (SEM and TEM) of parent and treated supports support were carried out in a Hitachi, models S400 (SEM) and H-8100 (TEM) microscopes. Textural characterization of the supports and **Fe** loaded samples was performed by N_2 adsorption isotherms at −196 °C in an automatic apparatus Micromeritics ASAP 2010. Before the isotherms acquisition the samples (≈50 mg) were outgassed at 150 °C, under vacuum better than 10^{-2} Pa for 2 h, in the case of supports and fresh catalysts, and for 17 h when used catalysts were analyzed.

Catalytic Tests of Fresh and Re-Used Samples

In a typical experiment, acetonitrile (3 mL), cyclohexane (5.00 mmol), **Fe** or **Fe**@Y B (5–20 μmol based on the iron complex, 0.1–0.4 mol% *vs.* substrate) and nitromethane (as internal standard, 50 μL) were introduced into a 25 mL Pyrex tube of a 10-way OmniStation Electrothermal MKII reactor. The promoter (if any) was then added and the reaction started with the addition of H_2O_2 (50% aqueous solution, 10.0 mmol) in a portion. The reaction mixture was stirred (800 rpm) at 25 °C for the desired times (4.5–72 h). After the reaction, the obtained mixture was centrifuged to separate the catalyst and a sample (4 μL) was taken from the organic phase and analyzed by GC or GC–MS.

Chromatographic analyses were undertaken by using a Fisons Instruments GC 8000 series gas chromatograph with a DB-624 (J&W) capillary column (DB-WAX, column length: 30 m; internal diameter: 0.32 mm), FID detector, and the Jasco-Borwin v.1.50 software. The temperature of injection was 240 °C. The initial temperature was maintained at 100 °C for 1 min, then raised 10 °C/min to 180 °C and held at this temperature for 1 min. Helium was used as the carrier gas. The products were identified by comparison of their retention times with known reference compounds. The internal standard method was used to quantify the organic products. The obtained values of conversion are the result of two concordant assays. GC-MS analyses were performed using a Perkin Elmer Clarus 600 C instrument (Helium as the carrier gas), equipped with two capillary columns (SGE BPX5; 30 m × 0.32 mm × 25 mm), one having an EI-MS (electron impact) detector and the other one with a FID detector. Reaction products were identified by comparison of their retention times with known reference compounds, and by comparing their mass spectra to fragmentation patterns obtained from the NIST spectral library stored in the computer software of the mass spectrometer.

Blank tests were performed, in a **Fe**-free system and no conversion of cyclohexane was detected.

Catalysts **Fe**@_Y_B recyclability was investigated for up to 3 consecutive cycles. After the first cycle, the supported catalyst was separated from the reaction mixture centrifugation followed by filtration, carefully washed with acetonitrile and dried at 80 °C overnight. Each consecutive cycle was initiated after the preceding one upon addition of new typical portions of all other reagents. After completion of each run, the products were analyzed as above-mentioned and the catalyst was recovered by centrifugation followed by filtration, thoroughly washed with acetonitrile, and dried in oven at 80 °C.

Hot filtration test: At an essay under the best reaction conditions, the immobilized **Fe** catalyst was removed from the reaction mixture by filtration using a hot frit, and the filtrate was monitored for continued activity. The results show that after removal of the catalyst, the reaction did not proceed, indicating that no catalytically active Fe compound remained in the filtrate.

Acknowledgements

Support for this work was provided by Fundação para a Ciência e Tecnologia through UID/MULTI/00612/2013, UID/QUI/00100/2013 and PTDC/QEQ-ERQ/1648/2014 projects.

Conflict of Interest

The authors declare no conflict of interest.

Keywords: scorpionate iron catalyst · hierarchical zeolite · oxidation · recyclable · cyclohexane

[1] P. Wu, P. Bai, Z. Yan, G. X. S. Zhao, *Sci. Rep.* **2016**, *6* 18817–18827.
[2] A. J. L. Pombeiro (Ed.), *Advances in Organometallic Chemistry and Catalysis*, John Wiley & Sons, Inc., Hoboken, NJ, USA, **2013**, Ch. 1–3 and 22.
[3] Metal-catalysis *in Industrial Organic Processes*, G. P. Chiusoli, P. M. Maitlis (Eds.), Royal Society of Chemistry, Cambridge, **2006**.
[4] J. Zhao, M. Zhu, J. Chen, Y. Yang, Y. Tang, Z. Cai, Y. Shen, C. He in *Fundamental of Chemical Engineering*, Pts 1–3, Vol. 233–235 (Eds.: Z.

Cao, L. Sun, X. Q. Cao, Y. H. H, TransTec Publications Inc, Zurich, **2011**, pp. 254–259;
[5] Ullmann's Encyclopedia of Industrial Chemistry, 6th ed., John Wiley and Sons, Inc. Online ISBN: 9783527306732.
[6] L. Que Jr., W. B. Tolman, *Nature* **2008**, *455*, 333–340.
[7] J. Luo, H. Yu, H. Wang, H. Wang, F. Peng, *Chem. Eng. J.* **2014**, *240*, 434–442.
[8] L. M. D. R. S. Martins, A. J. L. Pombeiro ,*Coord. Chem. Rev.* **2014**, *265*, 74–88.
[9] L. M. D. R. S. Martins, A. J. L. Pombeiro, *Eur. J. Inorg. Chem.* **2016**, 2236–2252.
[10] G. B. Shul'pin, *Catalysts* **2016**, *6*, 50–89.
[11] M. Sutradhar, L. M. D. R. S. Martins, M. F. C. Guedes da Silva, A. J. L. Pombeiro, *Coord. Chem. Rev.* **2015**, *301–302*, 200–239.
[12] L. M. D. R. S. Martins, *Catalysts* **2017**, *7*, 12–32.
[13] G. S. Mishra, E. C. B. A. Alegria, L. M. D. R. S. Martins, J. J. R. Fraústo da Silva, A. J. L. Pombeiro, *J. Mol. Catal. A* **2008**, *285*, 92–100.
[14] L. M. D. R. S. Martins, M. Peixoto de Almeida, S. A. C. Carabineiro, J. L. Figueiredo, A. J. L. Pombeiro, *ChemCatChem* **2013**, *5*, 3847–3856.
[15] M. Peixoto de Almeida, L. M. D. R. S. Martins, S. A. C. Carabineiro, T. Lauterbach, F. Rominger, A. S. K. Hashmi, A. J. L. Pombeiro, J. L. Figueiredo, *Catal. Sci. Technol.* **2013**, *3*, 3056–3069
[16] T. F. S. Silva, T. C. O. Mac Leod, L. M. D. R. S. Martins, M. F. Guedes da Silva, A. J. L. Pombeiro, *J. Mol. Cat. A: Chemical* **2013**, *367*, 52–60
[17] L. M. D. R.S Martins, A. Martins, E. C. B. A. Alegria, A. P. Carvalho, A. J. L. Pombeiro, *Appl. Catal. A* **2013**, *464–465*, 43–50.
[18] M. R. Maurya, A. Kumar, J. C. Pessoa, *Coord. Chem. Rev.* **2011**, *255*, 2315–2344.
[19] Y. Zhao, W. Lv, N. Lu, X. Shi, B. Fan, R. Li, *Microporous Mesoporous Mater.* **2018**, *257*, 35–41.
[20] T. Selvaraj, R. Rajalingam, V. Balasubramanian , *Appl. Surf. Sci.* **2018**, *434*, 781–786.
[21] H. W. Xing, X. W. Li, G. L. Tian, Y. H. Ye, *Tetrahedron* **2000**, *56*, 3517–3522.
[22] D. P. Serrano, J. M. Escola, P. Pizarro *Chem. Soc. Rev.* **2013**, *42*, 4004–4035.
[23] W. Schwieger, A. G. Machoke, T. Weissenberger, A. Inayat, T. Selvam, M..
[24] J. C. Groen, R. Caicedo-Realpe, S. Abelló, J. Pérez-Ramirez, *Mater. Lett.* **2009**, *63*, 1037–1040.
[25] J. C. Groen, J. A. Moulijn, J. Pérez-Ramirez, *J. Mater. Chem.* **2006**, *16*, 2121–2131.
[26] V. Paixão, A. P. Carvalho, J. Rocha, A. Fernandes, A. Martins, *Microporous Mesoporous Mater.* **2010**, *131*, 350–357.
[27] V. Paixão, R. Monteiro, M. Andrade, A. Fernades, J. Rocha, A. P. Carvalho, A. Martins, *Appl. Catal. A* **2011**, *402*, 59–68.
[28] J. Pérez-Ramírez, S. Abelló, A. Bonilla, J. C. Groen, *Adv. Funct. Mater.* **2009**,*19*, 164–172.
[29] V. Machado, J. Rocha, A. P. Carvalho, A. Martins, *Appl. Catal. A* **2012**, *445–446*, 329–338.
[30] A. P. Carvalho, N. Nunes, A. Martins in *Comprehensive Guide for Mesoporous Materials, Vol. 3: Properties and Development* (Ed.: Mahmood Aliofkhazraei) Nova Science Publishers, Inc. **2015**, pp. 147–211.8
[31] T. F. S. Silva, E. C. B. A. Alegria, L. M. D. R. S. Martins, A. J. L. Pombeiro, *Adv. Synth. Catal.* **2008**, *350*, 706–716.
[32] J. Garcia Martinez, M. Johnson, J. Valla, K. Li, J. Ying, *Catal. Sci. Technol.* **2012**, *2*, 987–994.
[33] J. Y. Ying, J. Garcia-Martinez, US Patent 7, 976, 696
[34] J. Garcia-Martinez, K Li, G. Krishnaiah, *Chem. Commun.* **2012**, *48*, 11851–11843.
[35] ASTM D3906–03, 2013. Standard test method for determination of relative X-ray diffraction intensities of Faujasite-type Zeolite-containing materials.
[36] M. Thommes, K. Kaneko, A. Neimark, J. Olivier, F. Rodriguez-Reinoso, J. Rouquerol, K. Sing, *Pure Appl. Chem.* **2015**, *87*, 1051–1069.
[37] S. J. Greeg, K. S. W. Sing, Adsorption, Surface Area and Porosity, Academic Press, second ed., London, 1982.
[38] Katie A. Cychosz, Rémy Guillet-Nicolas, Javier García-Martinez, Matthias Thommes, *Chem. Soc. Rev.* **2017**, *46*, 389–414
[39] G. B. Shul'pin, Y. N. Kozlov, G. V. Nizova, G. Süss-Fink, S. Stanislas, A. Kitaygorodskiy, V. S. Kulikova, *J. Chem. Soc. Perkin Trans.* **2001**, *2*, 1351–1371
[40] T. Yamashita, P. Hayes, *Appl. Surf. Sci.* **2008**, *254*, 2441–2449.
[41] M. Descostes, F. Mercier, N. Thromat, C. Beaucaire, M. Gautier-Soyer, *Appl. Surf. Sci.* **2000**, *165*, 288–302.
[42] D. L. Reger, T. C. Grattan, K. J. Brown, C. A. Little, J. J. S. Lamba, A. L. Rheingold, R. D. Sommer, *J. Organomet. Chem.* **2000**, *607*, 120–128.

Manuscript received: June 8, 2018
Accepted Article published: June 19, 2018
Version of record online: ■■, ■■■

FULL PAPERS

The right support porosity is the key for reusing: The catalytic performance and recyclability of iron (II) complex immobilized on hierarchical Y support was strongly affected by the textural properties of the support. NH_4OH treated support was able to retain the catalyst and a high catalytic performance is kept after three consecutive catalytic cycles.

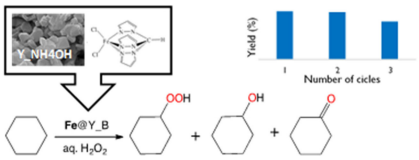

V. Van-Dúnem, Dr. A. P. Carvalho, Prof. L. M. D. R. S. Martins*, Dr. A. Martins**